WJPMR, 2026, 12(4), 142-154

Research Article

WORLD JOURNAL OF PHARMACEUTICAL AND MEDICAL RESEARCH

www.wjpmr.com

Impact Factor: 7.555

ISSN (O): 2455-3301

ISSN (P): 3051-2557

Coden USA: WJPMBB

DEVELOPMENT AND CHARACTERIZATION OF METRONIDAZOLE LOADED FRUIT-BASED NANOPARTICLES AND NANODRUGS

Ucheokoro Adaeze S.[1]*, Jackson Tenderwealth C.[2]

*[1]Department of Pharmaceutics and Pharmaceutical Technology, University of Port Harcourt, Port Harcourt 500004, Nigeria.

[2]Department of Pharmaceutics and Pharmaceutical Technology, University of Uyo, Uyo, 520003, Nigeria.

***Corresponding Author: Ucheokoro Adaeze S.**

Department of Pharmaceutics and Pharmaceutical Technology, University of Port Harcourt, Port Harcourt 500004, Nigeria.

DOI: https://doi.org/10.5281/zenodo.19327555

How to cite this Article: Ucheokoro Adaeze S.[1]*, Jackson Tenderwealth C.[2] (2026). Development And Characterization Of Metronidazole Loaded Fruit-Based Nanoparticles And Nanodrugs. World Journal of Pharmaceutical and Medical Research, 12(4), 142–154.

Article Received on 28/02/2026 **Article Revised on 20/03/2026** **Article Published on 01/04/2026**

ABSTRACT

Background: The emergence of antimicrobial resistance and limitations associated with conventional dosage forms of metronidazole necessitate innovative drug delivery strategies. Green nanotechnology offers an eco-friendly approach to improving drug physicochemical properties and therapeutic performance.

Objective: This study aimed to develop and characterize metronidazole-loaded silver nanoparticles synthesized using aqueous fruit extracts of ***Carica papaya*** and ***Musa acuminata*** as natural reducing and stabilizing agents.

Methods: Fruit extracts were prepared by aqueous maceration and reacted with silver nitrate solution in the presence of metronidazole to produce nanoparticle formulations. The synthesized nanodrugs were evaluated for physicochemical properties (pH and solubility), morphology using Scanning Electron Microscopy (SEM), thermal behavior by Differential Scanning Calorimetry (DSC), functional group interactions through Fourier Transform Infrared Spectroscopy (FTIR), and optical properties using Ultraviolet–Visible (UV–Vis) spectroscopy.

Results: The formulations exhibited mildly acidic pH values (5.5–5.7) and were soluble in water, methanol, ethanol, dilute hydrochloric acid, chloroform, and acetone. SEM analysis revealed predominantly spherical nanoparticles with surface roughness, indicating increased surface area. DSC thermograms showed a reduction in melting point from 116 °C (pure metronidazole) to 88.5–91 °C in the nano-formulations, suggesting reduced crystallinity and successful drug incorporation. FTIR spectra confirmed the presence of hydroxyl and carbonyl groups, indicating phytochemical capping and drug–nanoparticle interactions. UV–Vis spectra displayed characteristic surface plasmon resonance bands between 272–407 nm, confirming silver nanoparticle formation and drug loading. **Conclusion:** Fruit-mediated green synthesis successfully produced stable metronidazole-loaded nanoparticles with modified physicochemical and structural properties, demonstrating potential for improved antimicrobial drug delivery.

KEYWORDS: Green synthesis, Silver nanoparticles, Metronidazole, Fruit extracts, Nanodrug characterization, Sustainable nanotechnology.

INTRODUCTION

The development and characterization of metronidazole-loaded fruit-based nanoparticles have emerged as a promising strategy in pharmaceutical nanotechnology, combining green synthesis principles with enhanced drug delivery for antimicrobial applications. Metronidazole, a nitroimidazole antibiotic, is widely used for treating anaerobic bacterial and protozoal infections, including periodontitis, giardiasis, and amoebiasis.[1,2] However, its clinical utility is limited by poor water solubility, bitter taste, short half-life (6–8 hours), gastrointestinal side effects, and the need for frequent dosing, which contributes to patient non-compliance and antimicrobial resistance.[3] To address these challenges, nanoparticle-based delivery systems offer sustained release, improved bioavailability, targeted delivery, and reduced toxicity.[4,5]

Fruit-based nanoparticles leverage natural phytochemicals (e.g., flavonoids, ascorbic acid, polyphenols) from fruits as reducing and capping agents, enabling eco-friendly synthesis without toxic chemicals.[6,7] This green approach aligns with sustainable development goals, reducing environmental impact while producing stable, biocompatible nanoparticles.[8,9] For instance, Bawazeer et al., developed gold nanoparticles (AuNPs) using black pepper (Piper nigrum) fruit extract, where polyphenols acted as reductants, yielding spherical particles of 20–50 nm with UV-Vis absorption at 530 nm.[8] FTIR analysis confirmed capping by O-H and C=O groups, while TEM and XRD verified morphology and crystallinity. Such fruit-mediated synthesis facilitates metronidazole loading by electrostatic adsorption or encapsulation, enhancing stability and controlled release.

Development processes typically involve extract preparation, nanoparticle synthesis, and drug loading. Hossain et al. used lemon fruit extract for zinc oxide nanoparticles (ZnONPs),[10] achieving 30 nm size with dynamic light scattering (DLS), polydispersity index (PDI) of 0.25, and zeta potential of -25 mV, indicating colloidal stability. SEM/EDX confirmed elemental composition, while FTIR showed capping by citrus compounds. Similar methods for metronidazole loading, as in Jahura et al. involved electrostatic adsorptive loading onto chitosan nanoparticles using ciprofloxacin as a co-drug, resulting in 80–90% encapsulation efficiency (EE) and prolonged release over 48 hours following the Higuchi model ($R^2 = 0.95$).[11] The fruit extract's antioxidants prevented aggregation, maintaining particle size <200 nm.

Characterization is essential to ensure nanoparticle quality, stability, and safety. Key techniques include UV-Vis spectroscopy for plasmon resonance, FTIR for functional groups, TEM/SEM for morphology, DLS for size/PDI/zeta, XRD for crystallinity, and HPLC for EE and release kinetics[11,12] Elzatahry and Eldin characterized metronidazole-loaded chitosan nanoparticles with TEM (100–200 nm), zeta potential (+35 mV), and EE >70%, showing sustained release via Fickian diffusion.[3] Cadinoiu et al. reported metronidazole-chitosan NPs with antimicrobial activity against Clostridium perfringens, with MIC reduced from 8 µg/mL to 4 µg/mL due to enhanced cellular uptake.[5]

Fruit-based systems enhance metronidazole's antimicrobial efficacy. Steckiewicz et al. evaluated silver NPs loaded with metronidazole, showing synergistic effects against periodontitis biofilms (MIC reduction 50–75%), with low cytotoxicity (<10% cell death at 50 µg/mL).[3] Pathak and Akhtar discussed nano-probiotics, noting fruit-capped NPs improve probiotic-metronidazole combinations for gut infections, with EE >85% and stability over 3 months.[13]

Despite advances, challenges include scalability, regulatory hurdles, and variability in fruit extracts.[6,7] Future development should focus on optimized loading (e.g., >90% EE) and *in-vivo* evaluation for periodontitis and invasive salmonellosis.[14,3]

MATERIALS AND METHODS

Materials

Collection of materials

Fresh fruits of *Musa acuminate* (banana) and *Carica papaya* (pawpaw) were obtained from a local farm in Amaokwe Achara, Uturu, Abia State, Nigeria. Aqueous extracts of the fruits were prepared using maceration method.

Method

Fruits Extraction Procedure

The fruits of *Carica papaya* (pawpaw) and *Musa acuminata* (banana) were thoroughly washed to remove dust and other debris. The water on the outer surface of the fruits was get-rid of and allowed to dry off at room temperature. Fruit(s) peeling was done using knife, size reduction of a 50 g weight of each fruit was carried out using fruit juice extractor and then about 200 mL aqueous extracts from the fruits was obtained by filtration method using Whatman filter papers, funnels and beakers. The resultant extracts were set apart for further processing into nanoparticles.

Green Synthesis of $AgNO_3$ Nanoparticles and Nanodrugs Formulations

Different batches of fruit-based nanoparticles and nanodrugs formulations comprising $AgNO_3$, respective fruit extract (*Carica papaya, and Musa acuminata)*, and metronidazole were prepared in accordance with the method of Jackson *et al.* (2019) with slight modification.

Physicochemical Characterization of the Synthesized Fruit-Based Silver Nanoparticles

a.pH

A 1g quantity of each of the generated fruit-based silver nanoparticles was dispersed in a 100 mL of deionized water and was tested with a pH handheld meter (Hanna, India), the readings were taken in triplicate and recorded.

b. Solubility

The solubility of 0.1g quantity of the respective samples of *Carica papaya* and *Musa acuminata*-based nanoparticles were carried out at room temperature and at 40^0C in water bath using 10 mL of water, ethanol, methanol, acetone, chloroform, n-hexane and dilute mineral acids such as nitric and hydrochloric acids, respectively.

Morphological Studies of Nanodrugs Samples

Scanning Electron Microscopy (SEM)

The scanning electron microscopy (SEM) was performed to examine the physical structural change of nanodrug samples using Scanning Electron Microscope, model Phenom ProX, by phenom World Einhoven,

Netherlands. Sample was placed on double adhesive which was on a sample stub, was coated by quorum technologies model Q150R, with 5nm of gold. Thereafter it was taken to the SEM machine chamber where it was viewed through NaVCaM for focusing and little adjustment. It was then transferred to SEM mode, focused and brightness contrasting was automatically adjusted, afterward the morphology of different magnification was determined and obtained.

Differential Scanning Calorimetry (DSC)

A differential scanning calorimetry studies were carried out using a Differential Scanning Calorimetry machine (Mettler Toledo, model DSC 822, Switzerland). The nanodrug sample was thoroughly dried, to avoid damaging the equipment and about 5mg of the sample was weighed and placed in an aluminum pan pierced lid in atmosphere of liquid nitrogen at the rate of 20 mL / minute within the temperature range of 27- 400 ^{o}C at 10 ^{o}C rise/minute at incremental rate to generate the thermograms for the nanodrug samples.

Fourier Transform-Infrared Spectroscopy (FTIR)

About 10 mg quantity each of nanodrug samples was placed on a plate and sample pellets were formed. A smear was made and then sample alignment was determined (the blue lines were checked changed from red to green region). This was done and the nanodrug samples were placed for coding for peak determination, and the machine was set to pick the peaks, the peaks were selected and were properly labelled. FTIR analysis was carried out using Shimadzu FTIR, Model IR Affinity-1.

Determination of surface Plasmon resonance of Nanodrugs using Ultraviolet–Visible Light Absorption Spectroscopy

A 0.5 mg quantity each of nanodrugs samples was dissolved in 10 mL of distilled water, a 1 mL of the dissolved nanodrug was then placed in a spectralon plate of the UV/Visible instrument (PerkinElmer Lambdas 650-1050), fitted with a 150 mm center mount integrating sphere. The instrument background was then corrected and the nanodrug samples spectra and surface resonance were determined in scatter transmission and center mount mode.

Statistical Analysis

Statistical software called statistical package for the social science (SPSS) version 20 was used statistically to analyze the generated data.

RESULTS AND DISCUSSION

Results

Physicochemical Properties of the Synthesized Fruit-Based Silver Nanoparticles

pH

Table 1 below shows the pH values of *Carica papaya* and *Musa acuminata* nanoparticles.

Table 1: The pH values of *Carica papaya* and *Musa acuminate.*

Samples	pH
Carica papaya	5.7
Musa acuminata	5.5

Carica papaya and *Musa acuminata* fruit extracts served as reducing agent. Reportedly, it was observed that the surface plasmon resonance (SPR) peaks for acidic nanoparticles appeared at a relatively short wavelength of around, 330 nm.

Solubility

Carica papaya and *Musa acuminata*-based nanoparticles were soluble in water, ethanol, methanol, dilute HCl, chloroform and acetone. *Carica papaya* and *Musa acuminata* based nanoparticles were soluble in water, ethanol, methanol, dilute HCl, chloroform and acetone due to water soluble nature of the fruits used for green synthesis. This property enhances the dissolution rate and bioavailability of nanomedicines.

Scanning Electron Microscopy (SEM) Results of Metronidazole-loaded Fruit-Based Nanodrug

Scanning Electron Micrograph of Metronidazole-Loaded *Carica Papaya*-Based Nanodrug

Figures 1-2 below illustrate the scanning electron micrograph of metronidazole-loaded *Carica papaya*-based nanodrug.

Figure 1: SEM (micrograph) of PM1b.

Key: PM; P - Pawpaw (*Carica papaya*), M- Metronidazole, 1 – 1st dose of metronidazole pure sample (50 mg), b – 5.0 % w/v of $AgNO_3$ (2nd concentration of silver nitrate).
PM is a sample batch of metronidazole-loaded *Carica papaya*–based nanodrug.

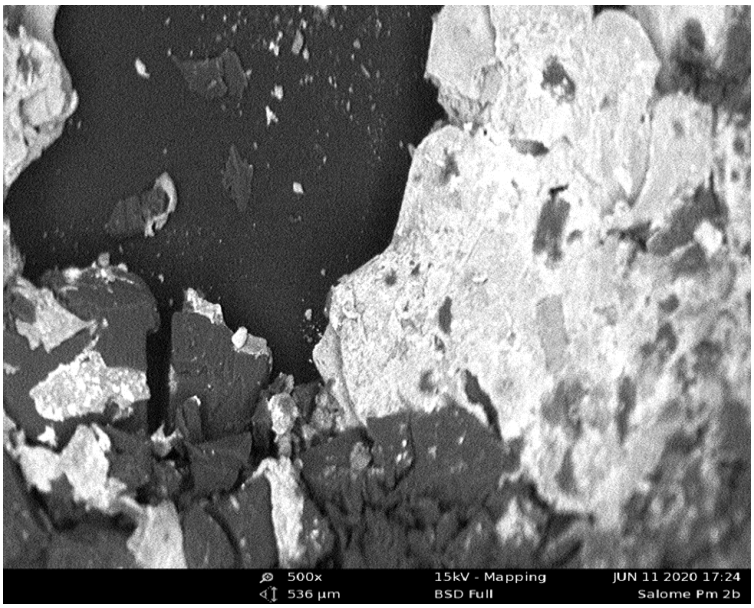

Figure 2: SEM (micrograph) of PM2b.

Key: PM; P - Pawpaw (*Carica papaya*), M - Metronidazole, 2 – 2nd dose of metronidazole pure sample (100 mg), b – 5.0% w/v of $AgNO_3$ (2nd concentration of silver nitrate).
PM is a sample batch of metronidazole-loaded *Carica papaya*–based nanodrug.

Scanning Electron Micrograph of Metronidazole-Loaded *Musa acuminata*-Based Nanodrugs
Figures 3-4 below illustrate the scanning electron micrograph of metronidazole-loaded *Musa acuminata*-based nanodrugs.

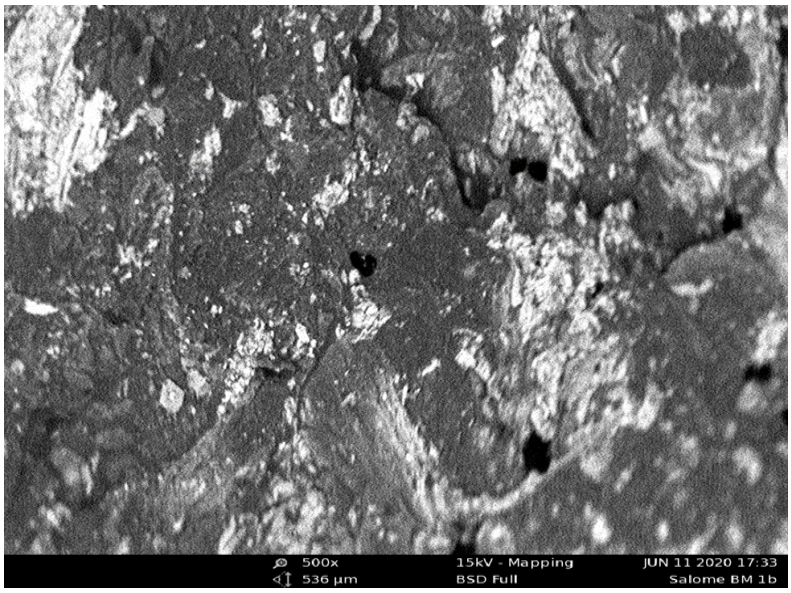

Figure 3: SEM (micrograph) of BM1b.

Key: BM; B - Banana (*Musa acuminata*), M - Metronidazole, 1 – 1st dose of metronidazole pure sample (50 mg), b – 5.0% w/v of $AgNO_3$ (2nd concentration of silver nitrate).
BM is a sample batch of metronidazole-loaded *Musa acuminata*–based nanodrug.

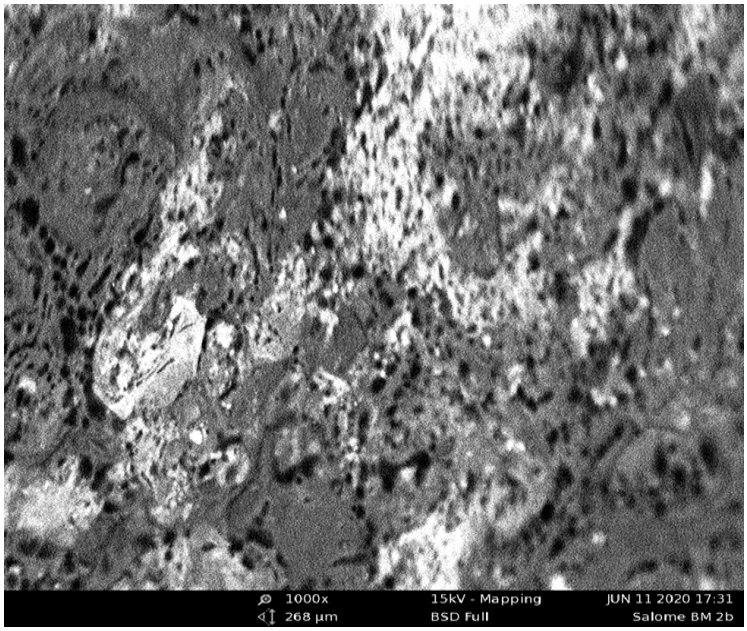

Figure 4: SEM (micrograph) of BM2b.

Key: BM; B - Banana (*Musa acuminata*), M - Metronidazole, 2 – 2nd dose of metronidazole pure sample (100 mg), b – 5.0% w/v of $AgNO_3$ (2nd concentration of silver nitrate). BM is a sample batch of metronidazole-loaded *Musa acuminata*–based nanodrug.

Scanning Electron Micrograph of Metronidazole Pure Sample

Figure 5: below illustrates the scanning electron micrograph of metronidazole pure sample.

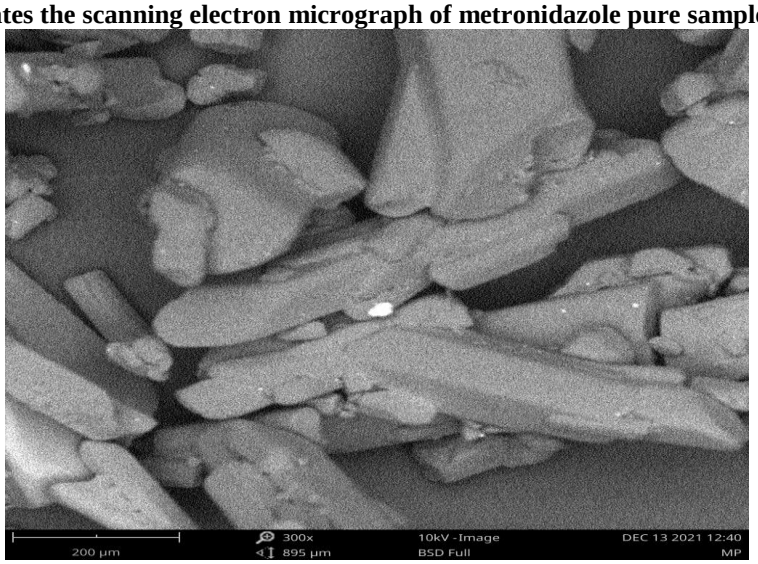

Figure 5: SEM (micrograph) of Metronidazole Pure Sample.

The micrographs (SEM) of metronidazole loaded fruit-based nanodrugs and its pure sample are respectively shown in figures 1 to 5 and it was shown that synthesized nanodrugs appeared as spherical colloidal nanoparticles.). The samples morphology showed that the nanoparticles had a certain degree of surface roughness. The ridges and surface roughness enhances and causes an increase in contact surface, contributing to more (increased) number of active sites on the colloidal surface of the nanoparticles which therefore, causes an increase in the surface area available for enzyme immobilization (nanoparticles mechanism of action).

Thermal Analysis (Differential Scanning Calorimetry, DSC) of Metronidazole-Loaded Fruit-Based Nanodrugs

Thermogram of Metronidazole-Loaded *Musa acuminata and Carica papaya*-Based Nanodrugs, Respectively

Figure 6 illustrates the thermogram of metronidazole-loaded *Musa acuminata and Carica papaya*-based nanoparticles, respectively.

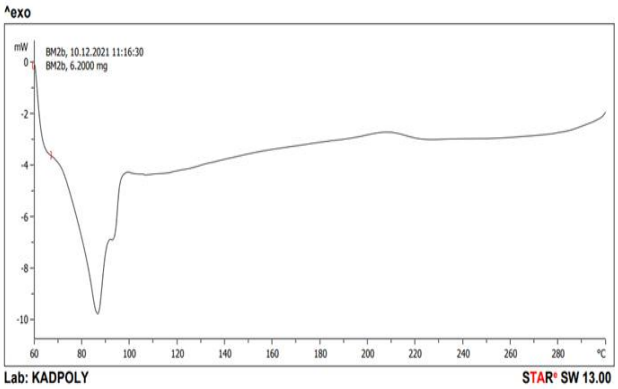

Figure 6: DSC Thermogram of BM2b.

Key: BM; P – Banana (*Musa acuminata*), M - Metronidazole, 2 – 2nd dose of metronidazole pure sample (100 mg), b – 5.0% w/v of $AgNO_3$ (2nd concentration of silver nitrate).

BM is a sample batch of metronidazole-loaded *Musa acuminata*–based nanodrug.

BM2b showed a melting point of 88.5 ^{o}C

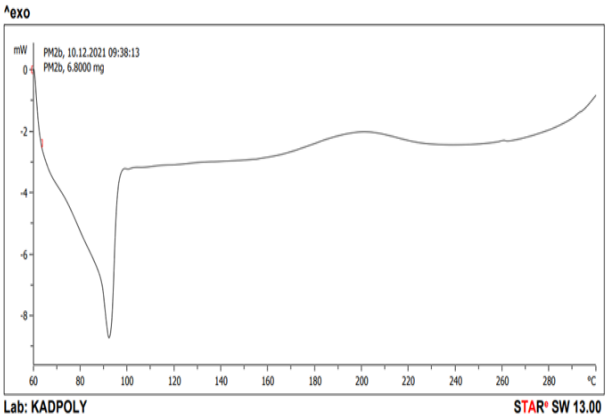

Figure 7: DSC Thermogram of PM2b.

Key: PM; P – Pawpaw (*Carica papaya*), M - Metronidazole, 2 – 2nd dose of metronidazole pure sample (125 mg), b – 5.0% w/v of $AgNO_3$ (2nd concentration of silver nitrate).

PM is a sample batch of metronidazole-loaded *Carica papaya*–based nanodrug.

PM2b showed a melting point of 91 ^{o}C.

Thermal Analysis (Differential Scanning Calorimetry, DSC) of Metronidazole Pure Sample

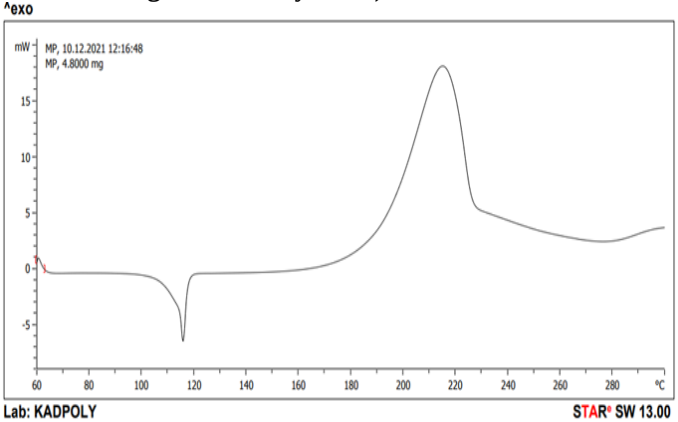

Figure 8: DSC Thermogram of Metronidazole Pure Sample.

Metronidazole pure sample showed a melting point of 116 ^{o}C.

The metronidazole-loaded-fruit-based nanodrugs displayed in figures 3.6 and 3.7 exhibited endothermic peak of 88.5 ^{o}C and 91 ^{o}C respectively, while in figure 3.8, metronidazole pure sample showed an endothermic peak of 116 ^{o}C. These endothermic peak ranges could be as a result of aqueous liquid loss during freeze drying which occurred within 6-6.75 min and exothermic peak of above 210 was obtained within 4.5-4.54 min which may be as a result of cross or recrystallization reaction and thermal decomposition of silver nanoparticles.

Fourier Transform InfraRed Spectroscopy (FTIR) Results of Metronidazole-Loaded Fruit-Based Nanodrugs
FTIR Spectroscopy of *Carica Papaya*-Based Metronidazole Nanoparticles
Figures 9-11: show the FTIR spectroscopy of *Carica papaya*-based metronidazole nanodrugs.

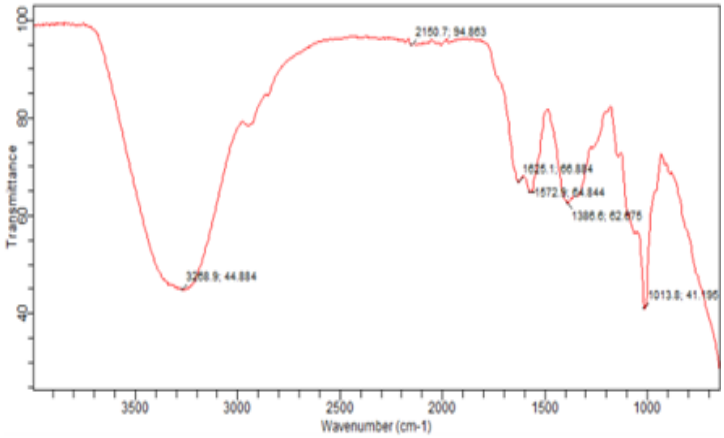

Figure 9: FTIR of PM1b.

Key: PM; P – Pawpaw (*Carica papaya*), M - Metronidazole, 1–1st dose of metronidazole pure sample (50 mg), b – 5.0 % w/v of $AgNO_3$ (2nd concentration of silver nitrate). PM is a sample batch of metronidazole-loaded *Carica papaya*–based nanoparticle.

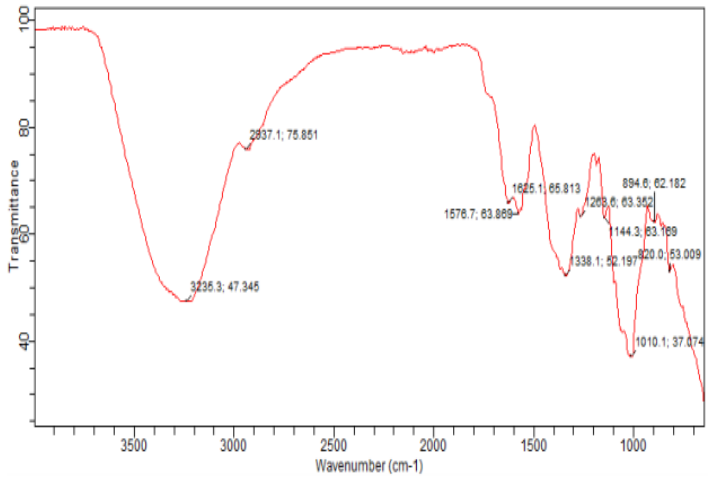

Figure 10: FTIR of PM2b.

Key: PM; P – Pawpaw (*Carica papaya*), M - Metronidazole, 2–2nd dose of metronidazole pure sample (100 mg), b – 5.0 % w/v of AgNO3 (2nd concentration of silver nitrate). PM is a sample batch of metronidazole-loaded *Carica papaya*–based nanoparticle.

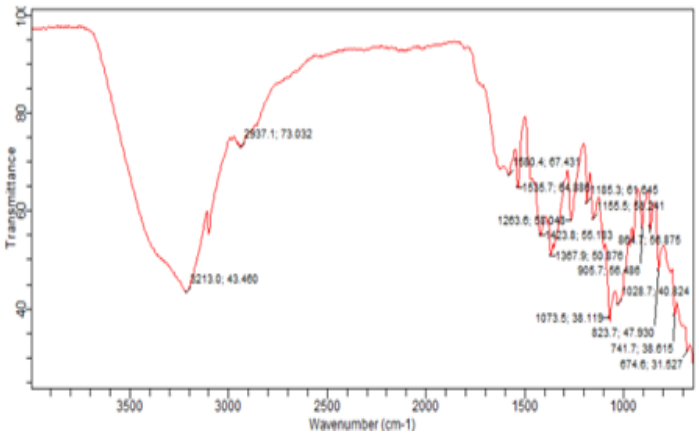

Figure 11: FTIR of PM3a.

Key: PM; P – Pawpaw (*Carica papaya*), M - metronidazole, 3–3rd dose of metronidazole pure sample (50 mg), a – 2.5 % w/v of $AgNO_3$ (1st concentration of silver nitrate).

PM is a sample batch of metronidazole-loaded *Carica papaya*–based nanoparticle.

FTIR Spectroscopy of *Musa acuminata*-Based Metronidazole Nanodrugs

Figures 12-14 illustrate the FTIR spectroscopy of *Musa acuminata*-based metronidazole nanodrugs.

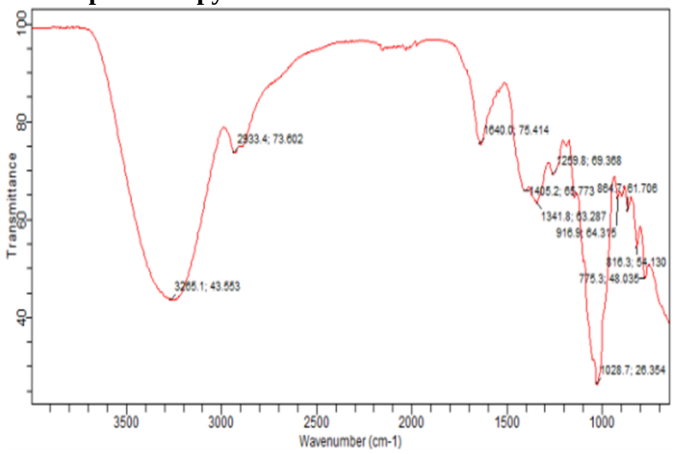

Figure 12: FTIR of BM1b.

Key: BM; B – Banana (*Musa acuminata*), M - Metronidazole, 1–1st dose of metronidazole pure sample (50 mg), a – 2.5 % w/v of $AgNO_3$ (1st concentration of silver nitrate).

BM is a sample batch of metronidazole-loaded *Musa acuminata*–based nanoparticle.

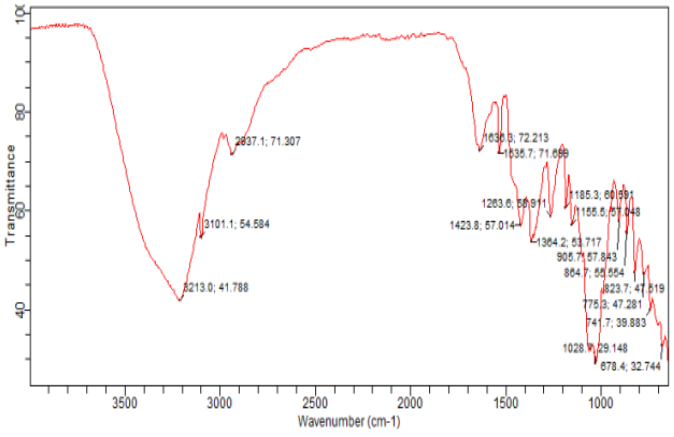

Figure 13: FTIR of BM2b.

Key: BM; B – Banana (*Musa acuminata*), M - Metronidazole, 2 – 2nd dose of metronidazole pure sample (100 mg), b – 5.0% w/v of $AgNO_3$ (2nd concentration of silver nitrate). BM is a sample batch of metronidazole-loaded *Musa acuminata*–based nanoparticle.

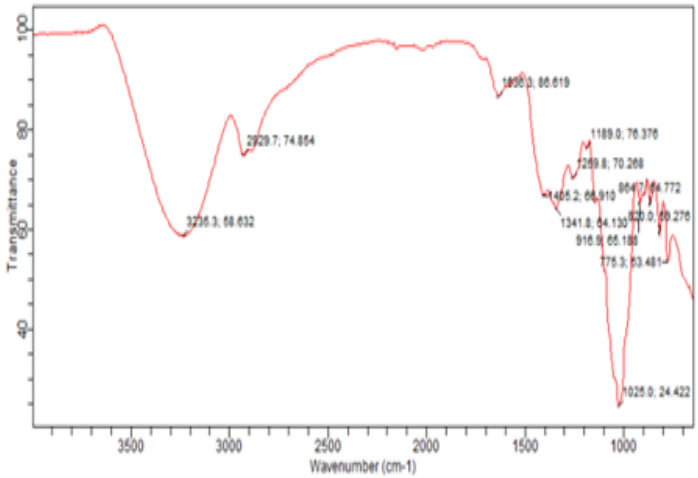

Figure 14: FTIR of BM3a.

Key: BM; B – Banana (*Musa acuminata*), M - Metronidazole, 3–3rd dose of metronidazole pure sample (200 mg), a – 2.5 % w/v of AgNO*3* (1st concentration of silver nitrate). BM is a sample batch of metronidazole-loaded *Musa acuminata*–based nanoparticle.

FTIR Spectroscopy of Metronidazole Pure Sample

Figure 15 illustrates the FTIR spectroscopy of metronidazole pure sample

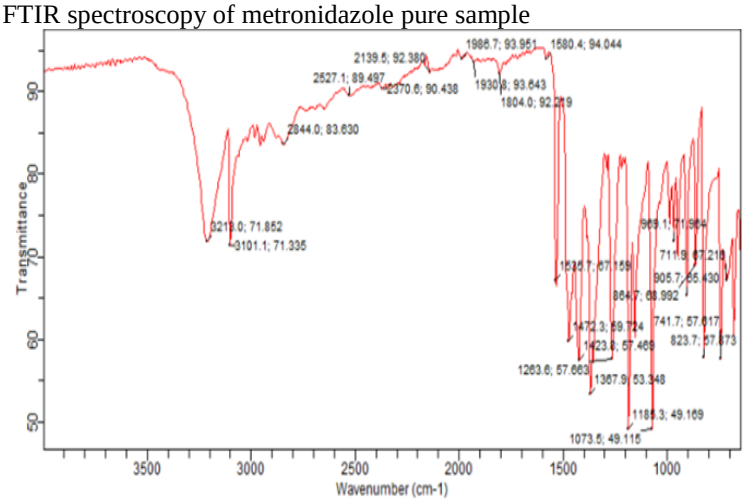

Figure 15: FTIR of Metronidazole Pure Sample.

Fourier Transmission Infrared Spectroscopy (FTIR) of the metronidazole pure sample in figure 15, showed broad band peak at 3218 cm^{-1}. While, in figures 14, metronidazole-loaded fruit-based nanodrugs showed broad bands peak at ranges of 3213 cm^{-1}–3265 cm^{-1} which is relative to the hydroxyl (-OH) group of phenol molecules. Additionally, these fruit-based nanodrugs also showed a broad band range of about 1535 which reportedly was proven to correspond with the carbonyl groups in amide linkages or stretching vibration of C=O group neighbour to C=C double bonds. There are other peaks which are between 675 cm^{-1} – 1018 cm^{-1}, relative to C=OH stretching of secondary alcohols, C-H aromatic compound and C-Cl alkyl halides, respectively (Ajitha *et al.*, 2015; Suarez-Cerda *et al.*, 2015).

Ultraviolet–Visible Light Absorption Spectroscopy Results of Metronidazole-Loaded Fruit-Based Nanodrugs

Ultraviolet–Visible Light Absorption Spectroscopy of *Carica papaya*-Based Metronidazole Nanoparticles

Figures 16-18 illustrate the ultraviolet–visible light absorption spectroscopy of *Carica papaya*-based metronidazole nanodrugs.

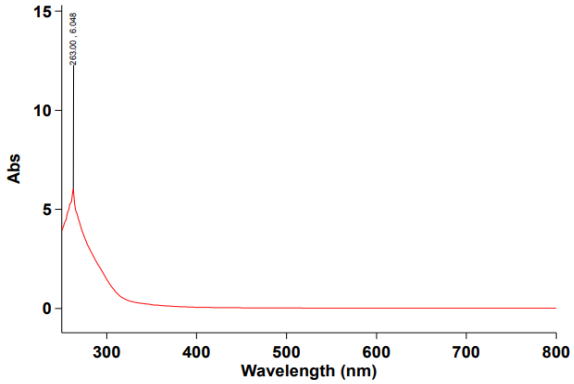

Figure 16: Ultraviolet – Visible Light Absorption Spectroscopy of PM1b.

PM1b showed a UV peak of 363 nm wavelength

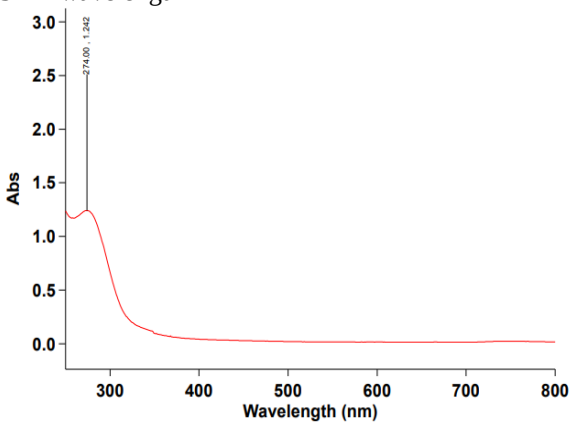

Figure 17: Ultraviolet – Visible Light Absorption Spectroscopy of PM2b.

PM2b showed a UV peak of 374 nm wavelength

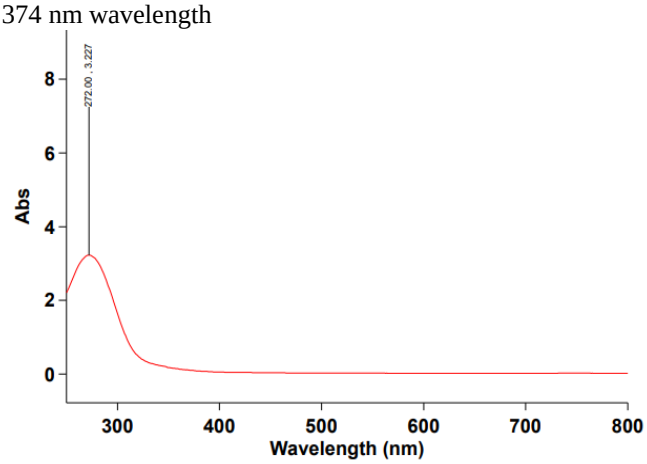

Figure 18: Ultraviolet – Visible Light Absorption Spectroscopy of PM3a.

PM3a showed a UV peak of 272 nm wavelength.

Ultraviolet–Visible Light Absorption Spectroscopy of *Musa acuminata*-Based Metronidazole Nanoparticles

Figures 19 and 20 illustrate the Ultraviolet–Visible Light Absorption Spectroscopy of *Musa acuminata*-based metronidazole nanoparticles**.**

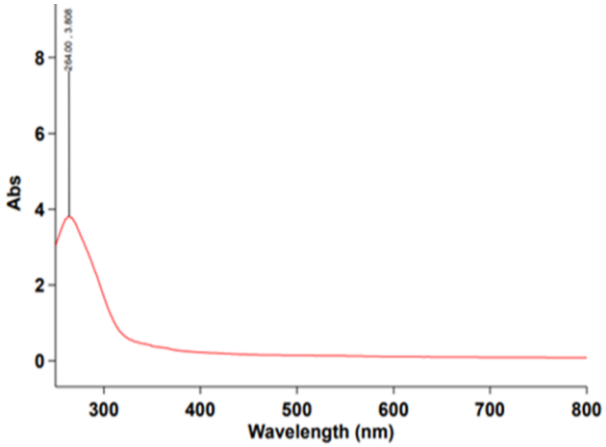

Figure 19: Ultraviolet – Visible Light Absorption Spectroscopy of BM1b.

BM1b showed a UV peak of 264 nm wavelength.

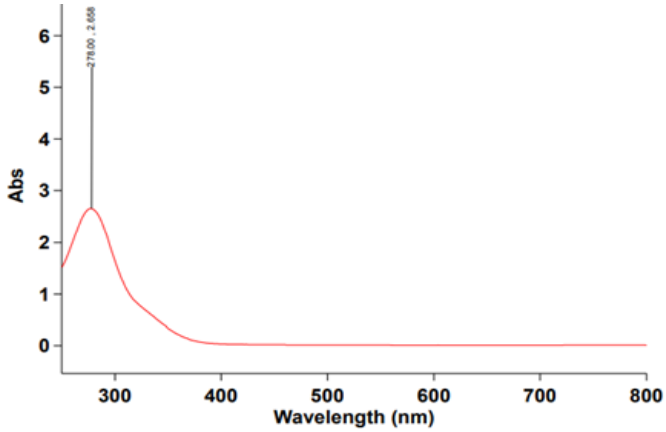

Figure 20: Ultraviolet – Visible Light Absorption Spectroscopy of BM3a.

BM3a showed a UV peak of 278 nm wavelength.

Ultraviolet–Visible Light Absorption Spectroscopy of Metronidazole Pure Sample

Figure 21 illustrates the Ultraviolet–Visible Light Absorption spectroscopy of Metronidazole pure sample.

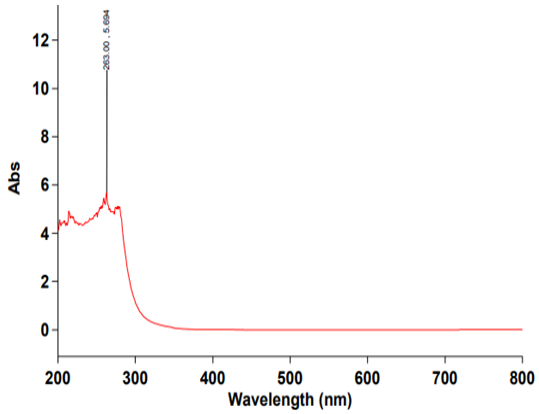

Figure 21: Ultraviolet – Visible Light Absorption Spectroscopy of Metronidazole Pure Sample.

Metronidazole pure sample showed a UV peak of 263 nm wavelength.

Figure 21 showed the respective UV-Vis spectra of metronidazole pure sample, at absorption band of 263 nm. While figures 16-20 showed UV-Visible spectra of the fruit-based nanodrugs. These spectra exhibited an absorption band at around 272–407 nm, where the absorbance upper limit (400- 407nm) was reported to be a typical plasmon band, which was as a result of the

formation of silver nanoparticles. In addition, the center of absorption band was an operating factor which was the nucleation controller and also possess a stabilizing property.

CONCLUSION

This study successfully developed metronidazole-loaded silver nanoparticles using aqueous extracts of Carica papaya and Musa acuminata as green reducing and stabilizing agents. The green synthesis approach produced stable fruit-based nanodrug formulations under mild experimental conditions without the use of toxic chemical reducing agents. Physicochemical evaluation showed that the synthesized nanoparticles possessed mildly acidic pH values (5.5–5.7), which are compatible with biological systems and may favor stability of silver nanostructures. Solubility studies demonstrated that the nanodrugs were soluble in water, ethanol, methanol, dilute hydrochloric acid, chloroform, and acetone, indicating improved dispersibility relative to the poorly water-soluble pure drug. Scanning Electron Microscopy (SEM) confirmed the formation of predominantly spherical colloidal nanoparticles with observable surface roughness. The roughened morphology suggests increased surface area, which is advantageous for drug adsorption and enhanced interaction with microbial membranes. In contrast, the pure metronidazole sample exhibited a distinctly different morphology, confirming structural modification following nano-formulation. Differential Scanning Calorimetry (DSC) analysis revealed a marked reduction in melting point of the nanodrug formulations (88.5–91 °C) compared to pure metronidazole (116 °C). This thermal shift indicates reduced crystallinity and possible amorphization of the drug within the nanoparticulate matrix, suggesting successful drug incorporation and improved physicochemical dispersion. Fourier Transform Infrared Spectroscopy (FTIR) confirmed functional group interactions between metronidazole, silver ions, and phytochemical constituents of the fruit extracts. Shifts in the hydroxyl and carbonyl stretching bands support the role of fruit phytochemicals as capping and stabilizing agents and confirm drug–nanoparticle interaction without destructive chemical alteration of the drug molecule. Ultraviolet–Visible spectroscopy demonstrated characteristic surface plasmon resonance bands between 272–407 nm, confirming the formation of silver nanoparticles. The observed spectral shifts relative to pure metronidazole (263 nm) further validate nanoparticle formation and successful drug loading.

Hence, the study establishes that fruit-based green synthesis is a viable and reproducible method for producing metronidazole-loaded silver nanoparticles with modified morphology, altered thermal behavior, confirmed functional group interactions, and characteristic plasmon resonance properties.

REFERENCES

1. Steckiewicz, K. P., Cieciórski, P., Barcińska, E., Jaśkiewicz, M., Narajczyk, M., Bauer, M.,... & Inkielewicz-Stepniak, I. (2022). Silver nanoparticles as chlorhexidine and metronidazole drug delivery platforms: Their potential use in treating periodontitis. *International Journal of Nanomedicine, 17*: 495–517.
2. Ovenseri, A. C., & Halilu, E. M. (2022). Formulation and in vitro evaluation of polymeric metronidazole nanoparticles. *Pakistan Journal of Pharmaceutical Sciences, 35*(5).
3. Elzatahry, A. A., & Eldin, M. M. (2008). Preparation and characterization of metronidazole-loaded chitosan nanoparticles for drug delivery application. *Polymers for Advanced Technologies, 19*(12): 1787–1791.
4. Arias, J. L., Martínez-Soler, G. I., López-Viota, M., & Ruiz, M. A. (2010). Formulation of chitosan nanoparticles loaded with metronidazole for the treatment of infectious diseases. *Letters in Drug Design & Discovery, 7*(2): 70–78.
5. Cadinoiu, A. N., Rata, D. M., Daraba, O. M., Atanase, L. I., Horhogea, C. E., Chailan, J. F., ... & Carauleanu, A. (2025). Metronidazole-loaded chitosan nanoparticles with antimicrobial activity against Clostridium perfringens. *Pharmaceutics, 17*(3): 294.
6. Kameswaran, S., Ramesh, B., Gopal, N. O., & Reddy, A. S. (2025). Plant-based nanoparticle synthesis. In *Plant-Based Nanoparticle Synthesis for Sustainable Agriculture* (pp. 20–29): CRC Press.
7. Hano, C., & Abbasi, B. H. (2021). Plant-based green synthesis of nanoparticles: Production, characterization and applications. *Biomolecules, 12*(1): 31.
8. Bawazeer, S., Khan, I., Rauf, A., Aljohani, A. S., Alhumaydhi, F. A., Khalil, A. A., ... & Khan, S. A. (2022). Black pepper (Piper nigrum) fruit-based gold nanoparticles (BP-AuNPs): Synthesis, characterization, biological activities, and catalytic applications—A green approach. *Green Processing and Synthesis, 11*(1): 11–28.
9. Haq, S. I., Nisar, M., Zahoor, M., Ikram, M., Islam, N. U., Ullah, R., & Alotaibi, A. (2023). Green fabrication of silver nanoparticles using Melia azedarach ripened fruit extract, their characterization, and biological properties. *Green Processing and Synthesis, 12*(1): 20230029.
10. Hossain, A., Abdallah, Y., Ali, M. A., Masum, M. M. I., Li, B., Sun, G., ... & An, Q. (2019). Lemon-fruit-based green synthesis of zinc oxide nanoparticles and titanium dioxide nanoparticles against soft rot bacterial pathogen Dickeya dadantii. *Biomolecules, 9*(12): 863.
11. Jahura, F. T., Ferdousi, F. K., Kamal, A. H. M., Ul-Hamid, A., Ehsan, M. Q., & Hossain, M. A. (2025). Electrostatic adsorptive loading of ciprofloxacin and metronidazole on chitosan nanoparticles to prolong the drug delivery process with preserved

antibacterial activities: Formulation and characterization. *Nanoscale Advances*, *7*(2): 621–633.
12. Arumugam, V., Subramaniam, S., & Krishnan, V. (2021). Green synthesis and characterization of zinc oxide nanoparticles using Berberis tinctoria Lesch. leaves and fruits extract of multi-biological applications. *Nanomedicine Research Journal*, *6*(3): 128–147.
13. Pathak, K., & Akhtar, N. (2018). Nanoprobiotics: Current trends and future prospects. In *Nanotechnology in Nutraceuticals* (pp. 123–145).
14. Jeon, H. J. (2023). Disease Surveillance and Implications on Public Health Decisions: Example of invasive Salmonellosis in invasive Salmonellosis in sub-Saharan Africa (Doctoral dissertation).